

Adsorption Behavior of Trimethylolpropane-Dehydroabiatic Acid Ester at the Air–water Interface

Juying Zhou^{1,2} · Yanping Yang¹ · Yuyan Liang¹ · Fuhou Lei^{1,2} · Haitang Xu^{1,2} · Jianfang Lu^{1,2} · Yanzhi Zhao^{1,2} · Yan Zhou¹

Received: 10 August 2015 / Accepted: 1 September 2016 / Published online: 12 September 2016
© AOCS 2016

Abstract A novel amphipathic trimethylolpropane-dehydroabiatic acid ester was successfully prepared with acyl chloride method. Various analytical techniques such as liquid chromatography–mass spectrometry, Fourier transform infrared spectrometry, proton and carbon nuclear magnetic resonance spectroscopy were employed to evaluate the chemical structure of the ester. The surface properties of the ester were investigated by surface tension and resonance light-scattering techniques. The surfactant molecules are adsorbed at the water–air interface in different adsorption states, i.e., state 1 and 2. The dynamic adsorption behavior was studied by combining experimental results and a reorientation model. The molar fraction of solvent decreased, while the molar fraction of surfactant molecules increased with increasing ester concentration at the surface layer. The adsorption value of state 1 presented a unimodal shape and the adsorption value of state 2 presented an s-shape with the increase in surface pressure. The free energy of adsorption is $-36.06 \text{ kJ mol}^{-1}$, more negative than the free energy of micellization ($-29.69 \text{ kJ mol}^{-1}$), it is actually easier for surfactant molecules to adsorb on the air–water interface.

Keywords Trimethylolpropane-dehydroabiatic acid ester · Surface property · Adsorption behavior · Free energy of adsorption

Introduction

Trimethylolpropane (TMP) is an important organic chemical intermediate with three primary hydroxyl groups. TMP is widely used in the fields of surfactants, high quality paints, plastics and the textile industry, etc. As a kind of polyol, TMP exhibits excellent reactivity, high molecular weight, high structure regularity as well as low glass transition temperature [1]. The hydroxyl groups can react with a carboxyl group to produce various esters. Biodegradable and environmentally acceptable esters for biodiesel, lubricants, solvents, surface active agents have been synthesized from vegetable oils and TMP. Linko *et al.* synthesized a polyol tri-ester using rapeseed oil fatty acid methyl and TMP by means of immobilized lipases without an additional organic solvent [2]. Zulkifli *et al.* described the transesterification process of TMP and palm oil [3], and they also stated that TMP is more thermally stable than glycerol [1]. In addition to the above-mentioned TMP esters, other esters such as a soybean oil–TMP ester [4], a *Jatropha curcas* oil–TMP ester and an oleic acid–TMP ester [5] have also been produced. The esterification processes were accomplished through transesterification reactions catalyzed by various enzymes [2, 6] or strong inorganic acids, aromatic acids, metal oxides, etc. [7].

Moreover, linear, comb and hyperbranched polyesters have been prepared from TMP. The formation of TMP-esters can eliminate the hydrogen molecules in the acids, improving the oxidative and thermal stability [8]. However, the monomers or chemical compounds that reacted

✉ Juying Zhou
zhoujuying@126.com

¹ School of Chemistry and Chemical Engineering, Guangxi University for Nationalities, Nanning 530006, People's Republic of China

² Guangxi Key Laboratory of Chemistry and Engineering of Forest Products, School of Chemistry and Chemical Engineering, Guangxi University for Nationalities, Nanning 530006, People's Republic of China

with TMP possess flexible structures, thus it can be expected that the products obtained from TMP and monomers with rigid structures will possess special properties. Rosin is an abundant natural product mainly obtained directly from the oleoresins of pines and conifers. The world total production of rosin is approximately 1.2 million tons annually. Rosin is a mixture of acidic (ca. 90 %) and neutral (ca. 10 %) compounds [9]. The acidic component, generally referred to as rosin acid, is a diterpenic monoacid with a rigid tricyclic hydrophenanthrene structure. The carboxyl group and the conjugated double bond in the structure impart high chemical reactivity to rosin [10, 11]. Therefore, rosin has been extensively used as a raw material for the preparations of various derivatives. Rosin and its ester derivatives are widely used in coating and microencapsulating agents [12–15].

To the best of our knowledge, a TMP based rosin ester has not been reported in the literature. In this study, we describe for the first time the synthesis of trimethylolpropane-dehydroabiatic acid ester. Because of the steric hindrance of the bulky phenanthrene moiety, the rosin esterification reactions take place at a high temperatures (>190 °C) or require prolonged reaction time, often in the presence of catalysts [16]. In order to avoid the drawbacks of the direct or the transesterification method, it is viable to apply a more effective method, i.e., acyl chloride method. It can yield high-purity products at lower temperatures by overcoming the steric hindrance of carboxyl groups on rosin.

This novel ester is expected to have special properties useful as surfactants or coating materials. The surface properties including critical micelle concentration (CMC), the aggregation behaviors, the minimum surface area of the molecule (A_{\min}), and the thermodynamic parameters of micellization and adsorption, etc. have been measured. It is essential to describe the adsorption process to interpret surface properties correctly. Reorientation theory has described quite well the equilibrium adsorption behaviors of a series of surfactants, such as oxyethylated alcohols, triton surfactants, alkyl dimethyl phosphine oxides [17–19]. In the present work, the novel trimethylolpropane-dehydroabiatic acid ester was synthesized and the surface properties were studied. The adsorption process of the surfactant was described with reorientation theory.

Experimental Procedures

Materials

Dehydroabiatic acid was purified to 98 % from disproportionated rosin that was produced by Wuzhou Chemicals, Guangxi province, China. Cyclohexane (AR) and

tetrahydrofuran (THF, AR) were refluxed with calcium hydride for 12 h, and then they were distilled and stored in amber glass bottles over molecular sieves (Kayou Type 4A). Trimethylolpropane (TMP, Aladdin, 98 %), 4-dimethylaminopyridine (DMAP, Adamas-beta, 99 %), Cellulose ester dialysis membranes (M1000, Union Carbide Corporation) were soaked in boiling distilled water for 30 min before being used.

Characterization Methods

The UV–Vis spectrum of the complex was recorded with the Shimadzu UV-1800 UV–Vis spectrophotometer.

HPLC experiments were carried out on an Agilent 1260-HPLC apparatus equipped with a Thermo Scientific C18 reversed-phase column (5 μm , 200 mm \times 4.6 mm). The mobile phase was potassium dihydrogen phosphate buffer solution (pH 3) and methanol (28:72). The detection wavelength was 215 nm, the column temperature was 35 °C and the flow rate was 1.0 mL min^{-1} .

The HPLC–ESI–MS (High Performance Liquid Chromatography Electrospray Ionization Multiple Mass Spectrometry) spectrum was run on a Shimadzu LCMS-2010A apparatus equipped with an ESI ion source, using methanol as solvent.

The FT-IR spectrum was obtained in the range of 400–4000 cm^{-1} using KBr discs on a Nicolet IS10 instrument.

The ^1H -NMR and ^{13}C -NMR spectra were recorded on a Bruker Avance (600/400) MHz spectrometer, using CDCl_3 as the solvent and TMS as the internal standard.

Resonance light scattering measurements were performed on a LS-55 Fluorescence Spectrophotometer (Perkin Elmer, America) equipped with a Xenon flash lamp, a photomultiplier detector, and dual monochromators. RLS spectra of the systems were recorded from 250 to 600 nm with synchronous scanning at $\lambda_{\text{ex}} = \lambda_{\text{em}}$ (i.e., $\Delta\lambda = 0$ nm).

Surface tensions were measured with a tensiometer BZY-2 (Shanghai, China) with a Wilhelmy plate at 25 °C.

Synthesis of Trimethylolpropane-Dehydroabiatic Acid Ester

Trimethylolpropane-dehydroabiatic acid ester was synthesized with the acyl chloride method. Dehydroabiatic acid (12 g, 40 mmol) was dissolved in cyclohexane (25 ml), and thionyl chloride (8 g, 60 mmol) was added slowly. After the solution was stirred at 85 °C for 4 h, excessive thionyl chloride and cyclohexane were removed by distillation. THF (20 ml), DMAP (4 g, 33 mmol) and TMP (24 g, 179 mmol) were subsequently added. The reaction mixture was stirred at room temperature overnight and then

washed with Na_2CO_3 solution, NaCl solution, and deionized water followed by drying over anhydrous Na_2SO_4 and evaporated to dryness. The product was further purified with silica gel chromatography (petroleum ether/ethyl acetate: 2.5/1 (v/v) to afford a white crystal product. $^1\text{H-NMR}$ (CDCl_3): δ (ppm): 7.17(d, $J = 8.1$ Hz, 1H, Ar), 7.01 (d, $J = 8.7$ Hz, 1H, Ar), 6.89 (s, 1H, Ar), 4.20 (s, 2H, COOCH_2), 3.59 (d, $J = 11.3$ Hz, 2H, OCH_2), 3.53 (d, $J = 11.3$ Hz, 2H, OCH_2), 2.95–1.77 (m, 14H), 1.59 (s, H_2O), 1.30 (s, 1H), 1.29 (s, 3H), 1.28 (s, 1H), 1.23 (s, 3H), 1.22 (s, 6H), 0.87 (dd, $J = 9.3, 5.9$ Hz, 3H). ^{13}C NMR (CDCl_3) δ (ppm): 179.74 (17), 146.63 (2), 145.75 (5), 134.45 (3), 126.94 (4), 124.13 (6), 123.99 (1), 65.85 (24), 65.83 (25), 64.36 (26), 48.09, 44.93, 43.00, 37.84, 36.98, 36.97, 33.42, 30.09, 25.33, 23.93, 22.53, 21.91, 18.55, 16.58, 7.37.

Surface Property Measured by RLS and Surface Tension

The stock solution of ester (9.62×10^{-6} mol L^{-1}) was prepared by dissolving 1 mg product in 250 mL water. The operating solutions were prepared by diluting the stock solutions with water. Prior to the experiments the solutions were incubated for at least 24 h at 25 °C. Each sample was put into a single-cell Peltier holder at 25 °C. After 20 min, the resonance light-scattering (RLS) spectra were measured by synchronous scanning at $\Delta\lambda = 0$ nm. The slit width was 2.5 nm/2.5 nm for all aqueous solutions of different concentrations. All the spectra were recorded at least three times to ensure perfect duplication.

Meanwhile, the surface tensions of the solutions were measured. All solutions of different concentrations were prepared and stored in closed bottles for 24 h before measurement. The platinum plate was always cleaned and heated to a red/orange color with a Bunsen burner before use. The aging time was at least 20 min.

Results and Discussions

Characterization of Trimethylolpropane-Dehydroabietic Acid Ester

FT-IR, ^1H NMR and ^{13}C NMR were performed to confirm the structure of trimethylolpropane-dehydroabietic acid ester. The FTIR spectra (Fig. 1b) show the typical, characteristic hydroxyl bands at 3440 cm^{-1} and the carbonyl band group (from ester) at 1724 cm^{-1} , consistent with the successful transformation of dehydroabietic acid into trimethylolpropane-dehydroabietic acid ester. The structure of the ester was further verified by ^1H NMR. The ^1H -NMR spectrum is shown in Fig. 2, there are broad singlets at

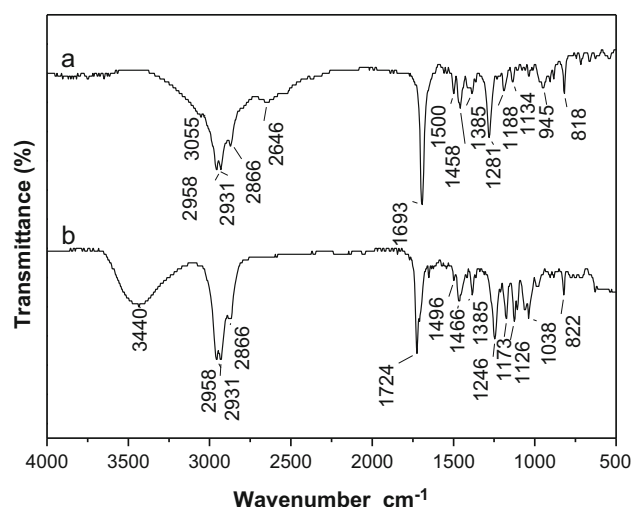


Fig. 1 IR spectra of dehydroabietic acid (a) and trimethylolpropane-dehydroabietic acid ester (b)

$\delta = 4.20$ ppm (proton of COOCH_2) and $\delta = 3.59$ ppm (proton of CH_2O). In addition, the characteristic bands at 8.87–7.16 ppm are attributed to the proton of phenyl. The ^{13}C -NMR spectrum in Fig. 3 further confirms the structure. In the ^{13}C -NMR spectrum, the chemical shift of phenyl carbon appears in the range of 123–147 ppm, and the chemical shift of carbon next to hydroxyl appears in the range of 64–69 ppm. The peak at 178.46 ppm is assigned to the carbonyl of the ester group. Formation of trimethylolpropane-dehydroabietic acid ester is also confirmed by high-resolution mass analysis. Observed HPLC–ESI–MS of the $[\text{M} + \text{Na}]^+$ and calculated values are in agreement with each other.

CMC Determination by Surface Tension and RLS Technologies

Figure 4a shows the RLS and the absorption spectra of trimethylolpropane-dehydroabietic acid ester aqueous solution at 25 °C. It can be seen that the ester exhibits two absorption peaks at 224 and 267 nm, which are attributed to the absorption of benzene and C=O group respectively. The absorbance is close to zero above 360 nm.

The RLS spectrum shows four scattering peaks, two strong peaks at 385 and 423 nm and two weak peaks at 326 and 485 nm. Resonance light scattering occurs when a scattering peak is near or within some absorption band of a scattering system [20]. Since the scattering peak at 326 nm overlaps the absorption band and the scattering peak at 385 nm is located near the absorption peak at 267 nm, both can be ascribed to RLS peaks. However, the scattering peaks at 423 and 485 nm appear on the red side of the absorption band where the absorbance approaches zero.

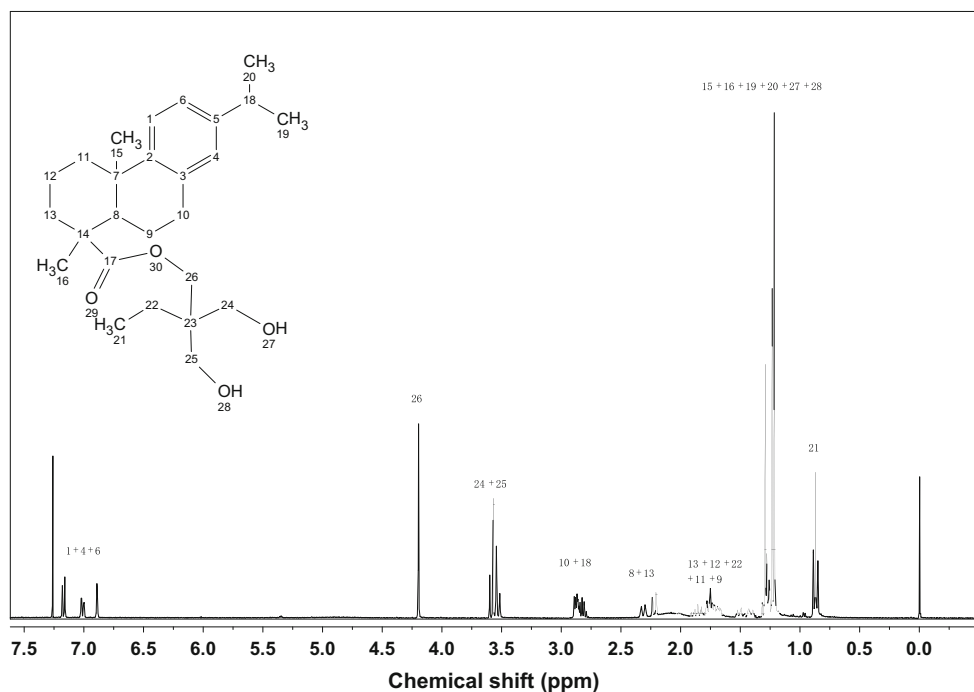


Fig. 2 ^1H -NMR spectrum of trimethylolpropane-dehydroabietic acid ester

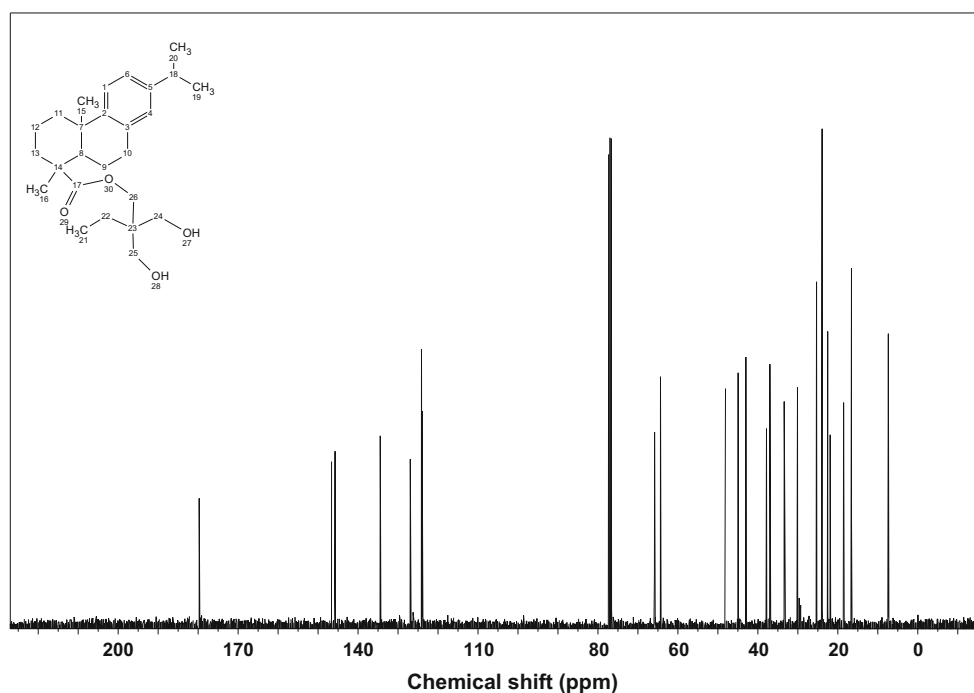


Fig. 3 ^{13}C -NMR spectrum of trimethylolpropane-dehydroabietic acid ester

Hence these two peaks are not ascribed to RLS but Rayleigh scattering. In the following, only the changes in RLS at 385 nm are investigated.

Figure 4b records the RLS spectra of trimethylolpropane-dehydroabietic acid ester aqueous solution with various concentrations ($0.96\text{--}9.61 \times 10^{-6} \text{ mol L}^{-1}$) at

25°C . In our experiment, the size of trimethylolpropane-dehydroabietic acid ester molecular is very small, far less than $1/10$ of the wavelength, thus the scattering below 385 nm can be regarded as resonance light scattering. It can be seen in Fig. 4b that the maximum intensities all appear at 385 nm, there is no peak shift and the RLS

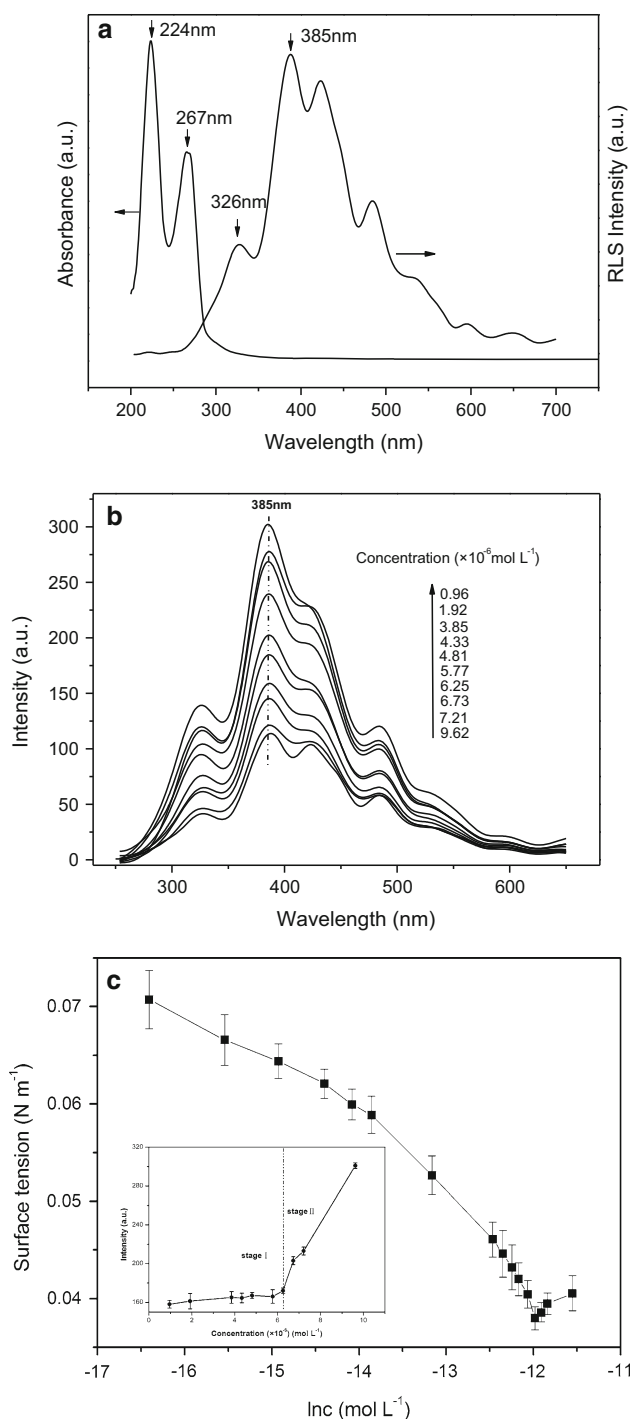


Fig. 4 **a** RLS and absorption spectra of trimethylolpropane-dehydroabiestic acid ester aqueous solution at 25 °C, **b** RLS spectra of trimethylolpropane-dehydroabiestic acid ester aqueous solutions with different concentrations ($0.96\text{--}9.61 \times 10^{-6} \text{ mol L}^{-1}$) at 25 °C, **c** Surface tension with different concentrations. The inset shows the concentration-dependence of the RLS intensities (I_{385})

intensity increases with increasing concentration. RLS intensity can be calculated using the following equation [21]:

$$\begin{aligned}
 I_{\text{RLS}}(\lambda) &= \frac{24\pi^3 v^2 n_{\text{med}}^4}{\lambda^4} \left| \frac{m^2 - 1}{m^2 + 2} \right|^2 \left(\frac{N}{V} \right) I_0(\lambda) \\
 &= \frac{24\pi^3 n_{\text{med}}^4 I_0(\lambda)}{\lambda^4} \left| \frac{m^2 - 1}{m^2 + 2} \right|^2 v^2 \left(\frac{c N_A}{V} \right) \\
 &= \frac{24 N_A \pi^3 n_{\text{med}}^4 I_0(\lambda)}{\lambda^4} \left| \frac{m^2 - 1}{m^2 + 2} \right|^2 c v^2 = K c v^2, \quad (1)
 \end{aligned}$$

where K is defined as

$$K = \frac{24 N_A \pi^3 n_{\text{med}}^4 I_0(\lambda)}{\lambda^4} \left| \frac{m^2 - 1}{m^2 + 2} \right|^2. \quad (2)$$

For fixed conditions and medium, K is constant. λ is the wavelength of incident light, $I_{\text{RLS}}(\lambda)$ is the resonance light scattering intensity of the ester aqueous solution, $I_0(\lambda)$ is the intensity of the incident light at λ , n_{med} is the refractive index of the medium, N/V is the number of the scattering particles per unit volume, v is the volume of one particle, c is the concentration of scattering particles, N_A is Avogadro's constant and m is the complex refractive index, respectively. It can be seen from Eq. (1) that the intensity of resonance light scattering depends on the concentration of the scattering particles and the volume of aggregates. Any changes in local density fluctuation and aggregates volume due to growth of concentration will change the RLS intensity.

The surface tension isotherm is shown in Fig. 4c. The inflection point in the isotherm corresponds to the critical micelle concentration (CMC). It is worth noting that trimethylolpropane-dehydroabiestic acid ester can significantly reduce the surface tension in water. Figure 4c also plots the concentration-dependent RLS intensity at 385 nm for various solution concentrations. With increasing concentration, the intensity I_{385} increases continually. I_{385} increases slightly at low concentration, and it increases sharply at high concentration. It is thought that the RLS intensity fluctuation can be briefly divided into two stages, i.e., stage I and stage II. In stage I, the scattering intensity increases almost linearly. Because at low concentrations (below $6.25 \times 10^{-6} \text{ mol L}^{-1}$), the scattering particles are single molecules and the volume of one particle v is invariable. It can be deduced that the increased intensity is attributed to the increase in concentration in Eq. 1. In stage II, a sharp increase in the scattering intensity appears. The slope increases, which suggests that the concentration contributes little to the intensity increment. Instead, aggregates with larger volume v must be formed at higher concentration (above $6.25 \times 10^{-6} \text{ mol L}^{-1}$) due to micelle formation. Meanwhile, the aggregation volume increases with concentration, because the aggregation number increases. Therefore, the inflection point in the concentration-intensity curve is also regarded as the CMC value of the amphipathic trimethylolpropane-dehydroabiestic acid ester solution.

These results also demonstrate the reliability of the RLS technique and its potential application in the surfactant field. It is observed that the CMC value of trimethylolpropane-dehydroabiatic acid ester is much lower than that of monomethyl PEG ester ($7 \times 10^{-5} \text{ mol L}^{-1}$) [22]. This phenomenon might be due to the strong hydrophobicity of trimethylolpropane-dehydroabiatic acid ester.

Simultaneous Adsorption of Different States at the Surface Layer

The equations of Gibbs, Butler, and Pethica are basic equations for deriving adsorption isotherms or equations of the state of an adsorption layer [23–25]. For nonideal behavior, different approximations are used in the literature based on the theories of regular solutions. The reorientation theory provides a reliable description of the behavior of surfactant molecules at the water–air interface. There are two kinds of molecules on the surface of water, i.e., water and surfactant molecules. The configuration states of surfactant molecules on the surface change with increasing concentration due to the asymmetry of surfactant molecules, leading to significant changes in various surface physical characteristics, such as CMC and surface tension. Therefore, the transition of surfactant molecule states reflects molecular motions or mechanisms of the transition. For simplicity, the surfactant molecules are assumed to be adsorbed onto the surface in two different states at different surface pressures ($\Pi = \gamma_0 - \gamma$). When $\Pi \approx 0 \text{ mN m}^{-1}$, the adsorption layer only consists of molecules in state 1 with maximum molar area ω_1 . When $\Pi > 30 \text{ mN m}^{-1}$, the adsorption layer consists only of molecules in state 2 with minimum molar area ω_2 . Therefore, the ω_{CMC} is identical to ω_2 [26]. For the non-ionic surfactant solution with a very dilute concentration, the adsorption value of surfactant at state 1, that is Γ_1 can be obtained from Eq. (3) derived from the Gibbs–Duhem formula [27] (Fig. 4c). The adsorption value at state 2, Γ_2 , can be obtained when the concentration is close to the CMC.

$$-\frac{d\gamma}{RT} = \Gamma d \ln a, \quad (3)$$

where, γ is the surface tension, R and T are the gas constant and temperature respectively, Γ is the adsorption value of the surfactant at the surface, a represents the activity of the surfactant in the solution. For dilute solutions ($<10^{-2} \text{ M}$), a can be replaced by the surfactant bulk concentration c , thus the equation can become

$$-\frac{d\gamma}{RT} = \Gamma d \ln c. \quad (4)$$

The partial molar surface area occupied by each adsorbed surfactant molecule can be calculated from Γ [28]:

$$\omega = \frac{1}{N_A \Gamma}, \quad (5)$$

where, N_A is the Avogadro constant. Combining Eqs. (4) and (5), the values of ω_1 and ω_2 of trimethylolpropane-dehydroabiatic acid ester molecules at the water–air interface can be obtained. ω_1 is $8.37 \times 10^5 \text{ m}^2 \text{ mol}^{-1}$, the molecular area in state 1 is 1.39 nm^2 . ω_2 is $1.81 \times 10^5 \text{ m}^2 \text{ mol}^{-1}$, the molecular area in state 2 is 0.3 nm^2 . The value of ω_1 is nearly equal to that of C_{10}EO_8 , while ω_2 value is lower than that of C_{10}EO_8 ($3.3 \times 10^5 \text{ m}^2 \text{ mol}^{-1}$). This phenomenon may be due to the different shapes and sizes of the hydrophobic sections of these two surfactants [18].

The molar fractions of solvent χ_0 , state 1 χ_1^s and state 2 χ_2^s change with surfactant concentrations and surface pressures [29].

$$\gamma_0 - \gamma = -\frac{RT}{\omega_0} \ln \chi_0^s = -\frac{RT}{\omega_0} (1 - \chi_1^s - \chi_2^s) \quad (6)$$

$$\ln \chi_0^s = -\frac{(\gamma_0 - \gamma) \omega_0 N_A}{RT}. \quad (7)$$

The surface area of the solvent ω_0 is a constant estimated from the molar area of a bulk-phase H_2O molecule, e.g., $\omega_0 = 10^5 \text{ m}^2 \text{ mol}^{-1}$ [30]. That is, the molecular area of solvent is 0.16 nm^2 . χ is the molar fraction, whose subscripts 0, 1 and 2 represent the solvent, state 1 and state 2 respectively. The superscript S indicates the surface phase. χ_0^s , χ_1^s and χ_2^s satisfy the following relation,

$$\chi_0^s + \chi_1^s + \chi_2^s = 1. \quad (8)$$

From Eqs. (6) and (8), χ_0^s and the sum of χ_1^s and χ_2^s can be obtained. It can be seen from Fig. 5, χ_0^s decreases with increasing Π or ester concentration, on the contrary, the sum of molar fractions of state 1 and 2, i.e., χ^s increases

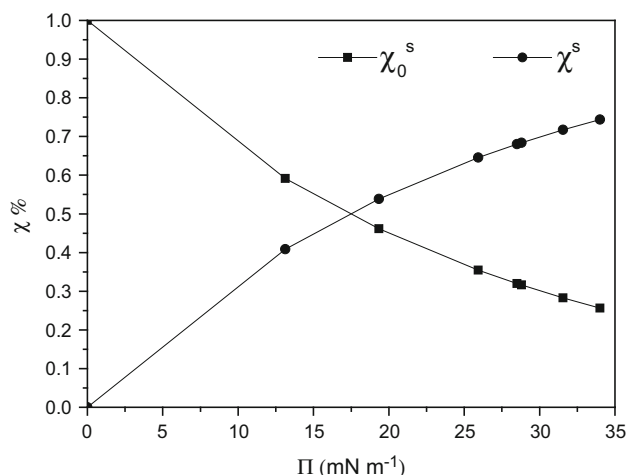


Fig. 5 Dependence of the molar fraction of solvent and trimethylolpropane-dehydroabiatic acid ester

with increasing Π due to the increase of trimethylolpropane-dehydroabiatic acid ester molecules at the water–air interface.

As a function of surface pressure, it should be noted that the values of Γ_1 and Γ_2 change with γ and Π in most cases except for two conditions ($\Pi \approx 0 \text{ mN m}^{-1}$ and $\Pi > 30 \text{ mN m}^{-1}$) due to the changes in the fraction of surfactant states. The ratio of molecules in the two possible adsorption states can be deduced from the generalized Joos adsorption equation [26],

$$\frac{\Gamma_1}{\Gamma_2} = \exp\left(\frac{\omega_1 - \omega_2}{\omega}\right) \left(\frac{\omega_1}{\omega_2}\right)^\alpha \exp\left[-\frac{\Pi(\omega_1 - \omega_2)}{RT}\right], \quad (9)$$

where, the total adsorption Γ and the mean molar area ω are defined by the following relations: $\Gamma = \Gamma_1 + \Gamma_2$, $\omega\Gamma = \omega_1\Gamma_1 + \omega_2\Gamma_2$. α is a constant related to the additional surface activity of state 1. For nonionic surfactants, $\alpha = 0$ [31]. Thus the Π - Γ_1 and Π - Γ_2 curves can be obtained. The dependence of adsorptions in state 1 and 2 on surface pressure is shown in Fig. 6.

From Fig. 6, it can be seen that Γ_1 first increases and then decreases with increasing Π . The Γ_1 curve presents a unimodal shape and the peak appears at about 5 mN m^{-1} . Meanwhile, it is observed that the Γ_1 value becomes constant when Π exceeds 30 mN m^{-1} . The Γ_2 curve presents an s-shape where the Γ_2 increases until Π reaches 30 mN m^{-1} . It is also discovered that Γ_1 is larger than Γ_2 when Π is below 5 mN m^{-1} . The Γ_2 begins to exceed Γ_1 when Π is higher than 5 mN m^{-1} . The variations of Γ_1 and Γ_2 reflect the change of the ratio of molecules in state 1 and 2, showing the evolution of molecular states. Similar results have been observed for C_{10}EO_8 surfactant [26].

The fraction of molecules χ_1^s and χ_2^s characterized by the particular value of partial molar area depend on the surface

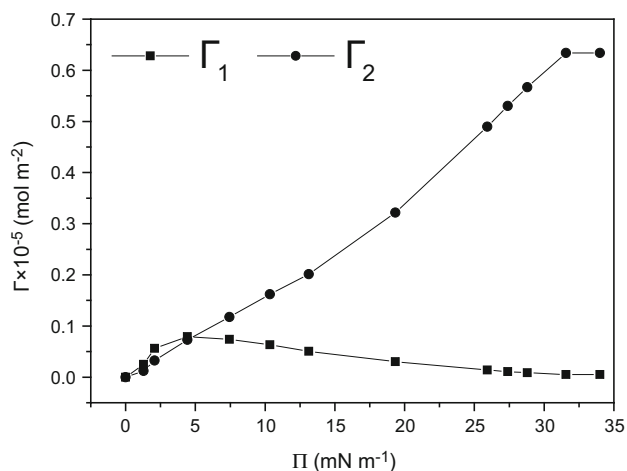


Fig. 6 Dependence of adsorption in state 1 (filled squares) and 2 (filled circles) on the surface pressure

pressure, and the ratio of the molar fractions of the two states in the surface layer following this equation [31].

$$\frac{\chi_2^s}{\chi_1^s} = K_{12} \exp\left[\frac{\Pi(\omega_1 - \omega_2)}{RT}\right], \quad (10)$$

where K_{12} is a constant, Π is the surface pressure; γ_0 and γ are the surface tensions of the solvent and the solution, respectively. If $\omega_1 > \omega_2$, the concentration of state 2 in the surface layer increases with the increase in Π . When $\Pi > 30 \text{ mN m}^{-1}$, the adsorption layer consists of molecules only in state 2. The transform of Eq. (10) is

$$\chi_1^s = \frac{\chi_2^s}{K_{12} \exp\left[\frac{\Pi(\omega_1 - \omega_2)}{RT}\right]}. \quad (11)$$

Here, χ_2^s is gradually increased. However, the detailed values cannot be obtained because K_{12} is unknown.

As can be seen in Fig. 7, with increased χ_2^s , χ_1^s firstly increases rapidly, and then χ_1^s falls to almost 0 and maintains constant at larger χ_2^s . The result verifies the accuracy and reliability of Fig. 6 from another point of view.

Free Energies of Adsorption and Micellization

ΔG_{mic} is the molar standard free energy of micellization of the surfactant, which is calculated by the equation valid for nonionic surfactants [32].

$$\Delta G_{mic} = RT \ln c_{CMC}, \quad (12)$$

where, the c_{CMC} is the critical micelle concentration. The molar free energy of adsorption ΔG_{ad} is calculated via the following equation:

$$\Delta G_{ad} = \Delta G_{mic} - 0.6023\Pi_{CMC}A_{min}, \quad (13)$$

where, $A_{min} = A_{CMC} = \omega_2 = 0.3 \text{ nm}^2$. ΔG_{mic} is equal to $-29.69 \text{ kJ mol}^{-1}$, indicating that the micellization process

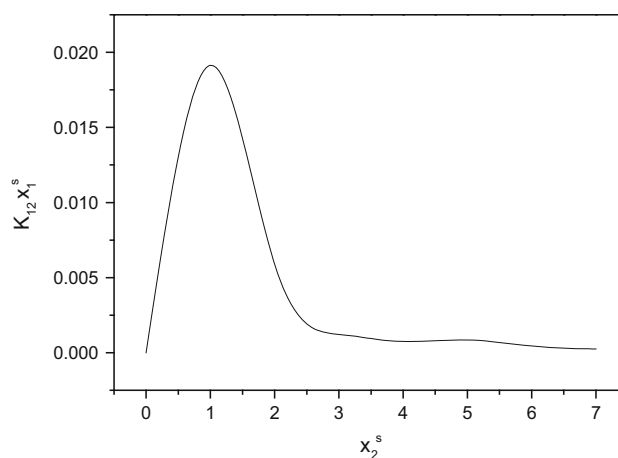


Fig. 7 Dependence of the χ_1^s on increasing χ_2^s

is spontaneous. ΔG_{ad} is $-36.06 \text{ kJ mol}^{-1}$, the value is more negative than ΔG_{mic} , demonstrating that the adsorption at the surface is associated with a decrease in the free energy of the system and the adsorption of trimethylolpropane-dehydroabiatic acid ester molecules on the surface is actually easier than micellization. This may be due to the steric effect of the phenanthrene ring inhibiting micellization more than on adsorption.

Conclusions

In conclusion, a novel trimethylolpropane-dehydroabiatic acid ester has been synthesized successfully. The ester was characterized with MS, FT-IR, $^1\text{H-NMR}$, and $^{13}\text{C-NMR}$ techniques. The CMC value was determined by the surface tension and RLS technologies. Reorientation model and experimental results were provided to explain the adsorption behavior of trimethylolpropane-dehydroabiatic acid ester molecules at the water–air interface as a function of concentration and surface pressure. The trimethylolpropane-dehydroabiatic acid ester molecules are adsorbed onto the surface in two different states. State 1 occupies the maximum molar area of ω_1 and state 2 has the minimum molar area ω_2 . The total molar fraction of two states increases with the increasing surface pressure, while the molar fraction of solvent decreases. The molar fraction of state 1 first increases and then decreases, the curve presents a unimodal curve. The molar fraction of state 2 increases and presents an s-shape curve. Furthermore, the free energy of adsorption is more negative than the free energy of micellization, which means that the adsorption of surfactant molecules on the surface is actually easier than micelle formation.

Acknowledgments We acknowledge the financial support from the program of National Natural Science Foundation of China (Grant No. 51203027, 21503043), Natural Science Foundation of Guangxi Province (Grant No. 2013GXNSFBA019035, 2015GXNSFCA139020), Scientific Research project of state ethnic affairs commission (Grant No. 14GXZ012), acknowledge Xiangsihu Young Scholars Innovative Research Team of Guangxi University for Nationalities.

References

1. Abu Bakar A, Yunus R, Chuah AL, Fakhru'l-Razi A (2007) Study on effect of hydroxyl group on lubrication properties of palm based trimethylolpropane Esters: Development of synthesis method. *J Appl Sci* 7:2011–2014
2. Linko Y, Tervakangas T, Lämsä M, Linko P (1997) Production of trimethylolpropane esters of rapeseed oil fatty acids by immobilized lipase. *Biotechnology* 11:889–892
3. Zulkifli NWM, Kalam MA, Masjuki HH, Shahabuddin M, Yunus R (2013) Wear prevention characteristics of a palm oil-based TMP (trimethylolpropane) ester as an engine lubricant. *Energy* 54:167–173
4. Bell EW, Cowan JC, Gast LE (1972) Potential lubricants for continuous casting of steel: polyol esters of partially hydrogenated soybean acids. *J Am Oil Chem Soc* 49:552–554
5. Arbain NH, Salimon J (2010) Synthesis and characterization of ester trimethylolpropane based *Jatropha curcas* oil as biolubricant base stocks. *J Sci Technol* 2:47–58
6. Kiriliauskaitė V, Bendikiene V, Juodka B (2011) Synthesis of trimethylolpropane esters of oleic acid by Lipoprime 50T. *J Ind Microbiol Biotechnol* 38:1561–1566
7. Itsikson TM, Milovidova NV, Rapport IB (1967) Esterification of trimethylolpropane with fatty acids. *Chem Technol Fuels Oils* 3:398–400
8. Yunus R, Fakhru'l-Razi A, Ooi TL, Iyuke SE, Idris A (2003) Preparation and characterization of trimethylolpropane esters from palm kernel methyl ester. *J Palm Res* 15:42–49
9. Ma Q, Liu X, Zhang R, Zhu J, Jiang Y (2013) Synthesis and properties of full bio-based thermosetting resins from rosin acid and soybean oil: the role of rosin acid derivatives. *Green Chem* 15:1300
10. Liu X, Zhang J (2010) High-performance biobased epoxy derived from rosin. *Polym Int* 59:607–609
11. Wang H, Liu X, Liu B, Zhang J, Xian M (2009) Synthesis of rosin-based flexible anhydride-type curing agents and properties of the cured epoxy. *Polym Int* 58:1435–1441
12. Fulzele SV, Satturwar PM, Dorle AK (2002) Polymerized rosin: Novel film forming polymer for drug delivery. *Int J Pharm* 249:175–184
13. Fulzele SV, Satturwar PM, Dorle AK (2002) Study of novel rosin-based biomaterials for pharmaceutical coating. *AAPS Pharm Sci Tech* 3:45–51
14. Kumar S, Gupta SK (2013) Rosin: a naturally derived excipient in drug delivery systems. *Polym Med* 43:45–48
15. Morkhade DM, Nande VS, Barabde UV, Patil AT, Joshi SB (2007) PEGylated rosin derivatives: novel microencapsulating materials for sustained drug delivery. *AAPS Pharm Sci Tech* 8:47
16. Maiti S, Ray SS, Kundu AK (1989) Rosin: a renewable resource for polymers and polymer chemicals. *Prog Polym Sci* 14:297–338
17. Miller R, Aksenenko EV, Liggieri L, Ravera F, Ferrari M, Fainerman VB (1999) Effect of the reorientation of oxyethylated alcohol molecules within the surface layer on equilibrium and dynamic surface pressure. *Langmuir* 15:1328–1336
18. Fainerman VB, Miller R, Aksenenko EV (2000) Adsorption behavior of oxyethylated alcohols at the solution/air interface. *Langmuir* 16:4196–4201
19. Fainermana VB, Lylyka SV, Aksenenko EV, Makievskic AV, Petkovd JT, Yorkee J, Millere R (2009) Adsorption layer characteristics of Triton surfactants 1. Surface tension and adsorption isotherms. *Colloids Surf A Physicochem Eng Asp* 334:1–7
20. Lu W (2006) Resonance light scattering and derived techniques in analytical chemistry: past, present, and future. *Microchim Acta* 158:29–58
21. Zhou JY, Yang J, Hu CL, Yang K, Zhang B, Chen XD (2011) Structure evolution and kinetics steps of the melting process of thermoreversible polymer gels. *Soft Matter* 7:5010–5019
22. Piispanen PS, Mikael Kjellin UR, Hedman B, Norin T (2003) Synthesis and surface measurements of surfactants derived from dehydroabiatic acid. *J Surf Deterg* 6:125–130
23. Adamson AW, Gast AP (1997) Physical chemistry of surfaces. Wiley, New York
24. Fainerman VB, Vollhardt D, Melzer V (1996) Equation of state for insoluble monolayers of aggregating amphiphilic molecules. *J Phys Chem* 100:15478–15482
25. Fainerman VB, Makievski AV, Vollhardt D, Siegel S, Miller R (1999) Equilibrium and dynamics of soluble surfactant penetration into a Langmuir monolayer of a 2D aggregating homologue. *J Phys Chem B* 103:330–337

26. Miller R, Fainerman VB, Möhwald H (2002) Adsorption behavior of oxyethylated surfactants at the air/water interface. *J Colloid Interface Sci* 247:193–199
27. Huang ZY, Zhang TL, Lu HC (2012) Surface and colloid chemistry. Petroleum Chemical Press, Beijing
28. Makievski AV, Fainerman VB, Bree M, Wustneck R, Kralgel J, Miller R (1998) Adsorption of proteins at the liquid/air interface. *J Phys Chem B* 102:417–425
29. Fainerman VB, Miller R, Wustneck R, Makievski AV (1996) Adsorption isotherm and surface tension equation for a surfactant with changing partial molar area 1 ideal surface layer. *J Phys Chem* 100:7669–7675
30. Fainerman VB, Zholob SA, Lucassen-Reynders EH, Miller R (2003) Comparison of various models describing the adsorption of surfactant molecules capable of interfacial reorientation. *J Colloid Interface Sci* 261:180–183
31. Fainerman VB, Lucassen-Reynders EH, Miller R (1998) Adsorption of surfactants and proteins at fluid interfaces. *Colloids Surf A Physicochem Eng Asp* 143:141–165
32. Rosen MJ (1989) Surfactants and interfacial phenomena. Wiley, New York

Juying Zhou obtained her Ph.D. at Sun Yat-Sen University in China in 2011. Currently, her research interests include synthesis of rosin-based polymers and surfactants.

Yanping Yang obtained her M.Sc. at Guangxi University for Nationalities in China in 2016. Currently, her research interests include synthesis of rosin-based polymers and confirmation transformation of polymer chains.

Yuyan Liang obtained her M.Sc. at Guangxi University for Nationalities in China in 2015. Currently, her research interests include synthesis of rosin-based polymers and confirmation transformation of polymer chains.

Fuhou Lei obtained his Ph.D. at Nanjing Forestry University in China in 2005. Currently, his research interests include synthesis of rosin-based polymers and molecular imprinting technology.

Haitang Xu obtained her M.Sc. at Guangxi University in China in 2008. Currently, her research interests include synthesis and drug loading on rosin-based polymers.

Jianfang Lu obtained her M.Sc. at Guangxi University in China in 2008. Currently, her research interests include synthesis of rosin-based polymers and enzyme immobilization.

Yanzhi Zhao obtained her M.Sc. at South China University of Technology in China in 2005. Currently, her research interests include synthesis of rosin-based polymers and confirmation transformation of polymer chains.

Yan Zhou obtained her Ph.D. at the University of Minnesota in 2010. Currently, her research interests include catalytic mechanisms of proteins with molecular dynamics simulations.